Conference Proceedings of the Society for Experimental Mechanics Series

Bonnie Antoun · H. Jerry Qi · Richard Hall · G.P. Tandon
Hongbing Lu · Charles Lu · Jevan Furmanski
Alireza Amirkhizi *Editors*

Challenges In Mechanics of Time-Dependent Materials and Processes in Conventional and Multifunctional Materials, Volume 2

Proceedings of the 2013 Annual Conference on Experimental and Applied Mechanics

SEM

Springer

Conference Proceedings of the Society for Experimental Mechanics Series

Series Editor
Tom Proulx
Society for Experimental Mechanics, Inc.,
Bethel, CT, USA

For further volumes:
http://www.springer.com/series/8922

Bonnie Antoun • H. Jerry Qi • Richard Hall • G.P. Tandon
Hongbing Lu • Charles Lu • Jevan Furmanski • Alireza Amirkhizi
Editors

Challenges In Mechanics of Time-Dependent Materials and Processes in Conventional and Multifunctional Materials, Volume 2

Proceedings of the 2013 Annual Conference on Experimental and Applied Mechanics

Springer

Editors
Bonnie Antoun
Sandia National Laboratories
Livermore, CA
USA

H. Jerry Qi
University of Colorado
Boulder, CO
USA

Richard Hall
Air Force Research Laboratory
Wright-Patterson AFB, OH
USA

G.P. Tandon
University of Dayton Research Institute
Dayton, OH
USA

Hongbing Lu
University of Texas-Dallas
Dallas, TX
USA

Charles Lu
University of Kentucky
Paducah, KY
USA

Jevan Furmanski
Los Alamos National Laboratory
Los Alamos, NM
USA

Alireza Amirkhizi
University California San Diego
La Jolla, CA
USA

ISSN 2191-5644 ISSN 2191-5652 (electronic)
ISBN 978-3-319-00851-6 ISBN 978-3-319-00852-3 (eBook)
DOI 10.1007/978-3-319-00852-3
Springer Cham Heidelberg New York Dordrecht London

Library of Congress Control Number: 2013945393

Printed on acid-free paper

Springer is part of Springer Science+Business Media (www.springer.com)

Preface

Challenges in Mechanics of Time-Dependent Materials and Processes in Conventional and Multifunctional Materials, Volume 2: Proceedings of the 2013 Annual Conference on Experimental and Applied Mechanics represents one of eight volumes of technical papers presented at the SEM 2013 Annual Conference & Exposition on Experimental and Applied Mechanics organized by the Society for Experimental Mechanics and held in Lombard, IL, June 3–5, 2013. The complete Proceedings also includes volumes on: *Dynamic Behavior of Materials; Advancement of Optical Methods in Experimental Mechanics; Mechanics of Biological Systems and Materials; MEMS and Nanotechnology; Experimental Mechanics of Composite, Hybrid, and Multifunctional Materials; Fracture and Fatigue; Residual Stress, Thermomechanics & Infrared Imaging, Hybrid Techniques and Inverse Problems*.

Each collection presents early findings from experimental and computational investigations on an important area within Experimental Mechanics, the Mechanics of Time-Dependent Materials and Processes being one of these areas.

This track was organized to address time (or rate)-dependent constitutive and fracture/failure behavior of a broad range of materials systems, including prominent research in both experimental and applied mechanics. Papers concentrating on both modeling and experimental aspects of time-dependent materials are included.

The track organizers thank the presenters, authors, and session chairs for their participation in and contribution to this track. The support and assistance from the SEM staff is also greatly appreciated.

Livermore, CA, USA — Bonnie Antoun
Boulder, CO, USA — H. Jerry Qi
Wright-Patterson AFB, OH, USA — Richard Hall
Dayton, OH, USA — G.P. Tandon
Dallas, TX, USA — Hongbing Lu
Paducah, KY, USA — Charles Lu
Los Alamos, NM, USA — Jevan Furmanski
La Jolla, CA, USA — Alireza Amirkhizi

Contents

Chapter 1
Micromechanics of the Deformation and Failure Kinetics of Semicrystalline Polymers

J.A.W. van Dommelen, A. Sedighiamiri, and L.E. Govaert

Abstract An elasto-viscoplastic two-phase composite inclusion-based model for the mechanical performance of semicrystalline materials has previously been developed. This research focuses on adding quantitative abilities to the model, in particular for the stress-dependence of the rate of plastic deformation, referred to as the yield kinetics. A key issue in achieving that goal is the description of the rate-dependence of slip along crystallographic planes. The model is used to predict time-to-failure for a range of static loads and temperatures. Application to oriented materials shows a distinct influence of individual slip systems.

Keywords Micromechanical modelling • Polyethylene • Semicrystalline polymers • Structure–property relation • Yield kinetics

1.1 Introduction

Both short and long-term failure of polymers are known to originate from usually rapid development of local irreversible (plastic) strain, manifesting itself in crazing and/or necking that ultimately results in loss of the structural integrity of the product. The mode of failure can be either brittle, characterized by fragmentation of the product, or ductile, involving the development of large localized plastic deformation zones accompanied by (more stable) tearing phenomena. The mode of failure and the time-scales on which they occur are strongly influenced by the molecular weight distribution of the polymer, the macromolecular orientation and the thermal history, i.e. factors that are directly connected to processing conditions. The latter is particularly true for semicrystalline polymers in which structural features, such as the degree of crystallinity, crystal type, size and orientation, that strongly influence their mechanical properties, may vary drastically depending on subtle details of the manner in which the polymer is shaped into the final product. In particular, shear flow significantly accelerates crystallization kinetics by increasing the amount of nuclei and generates an anisotropic morphology by inducing orientation.

The mechanical behaviour of semicrystalline polymeric materials, consisting of both amorphous and crystalline domains, depends strongly on the underlying microstructure (e.g. [1, 2]). Their elastic and viscoplastic behaviour depend on many factors such as the percentage crystallinity, the initial crystallographic and morphological texture and the mechanical properties of the individual phases. The ability to predict the mechanical properties of polymer products is uniquely linked to the capability to understand and predict the elasto-viscoplastic behaviour resulting from the underlying microstructure. Semicrystalline materials with oriented microstructures will behave anisotropically, which can play a crucial role in the performance and failure of polymer products.

Several experimental and modelling studies (e.g. [3–9]) have been dedicated to characterization and understanding of the viscoplastic behaviour and the evolution of texture of semicrystalline polymers. A previously developed micromechanically-based model for the constitutive behaviour of semicrystalline polymeric material [10] accounts for both crystallographic and morphological texture, the latter corresponding to the orientation distribution of the lamellar interface normals. The basic element in this model was a layered two-phase composite inclusion, comprising both a crystalline and an amorphous domain as developed by Lee et al. [6] for rigid viscoplastic semicrystalline materials.

J.A.W. van Dommelen (✉) • A. Sedighiamiri • L.E. Govaert
Department of Mechanical Engineering, Eindhoven University of Technology, P.O. Box 513, 5600 MB, Eindhoven, The Netherlands
e-mail: J.A.W.v.Dommelen@tue.nl

B. Antoun et al. (eds.), *Challenges In Mechanics of Time-Dependent Materials and Processes in Conventional and Multifunctional Materials, Volume 2*, Conference Proceedings of the Society for Experimental Mechanics Series,
DOI 10.1007/978-3-319-00852-3_1,

A three-level modelling approach was used to study intraspherulitic deformation and stresses for semicrystalline polyethylene [11] and to predict the response of tensile specimens obtained at different angles with respect to the extrusion direction of the material [12] in a qualitative sense.

The current research focuses on adding quantitative abilities to the micromechanical model, in particular for the stress-dependence of the rate of plastic deformation, referred to as the yield kinetics. A key issue in achieving that goal is the description of the rate-dependence of slip along crystallographic planes. The slip kinetics have been re-evaluated and characterized using a hybrid numerical/experimental procedure, based on the results for isotropic HDPE, loaded at various strain rates and temperatures. Because of the isotropy of the material, additional assumptions for the properties of these slip systems are required. Finally, the isotropically characterized model is applied to oriented polyethylene to investigate the potential of oriented system for characterizing the full slip kinetics of a semicrystalline polymer.

1.2 Model Description

The constitutive behaviour of semicrystalline material is modelled by an aggregate of two-phase composite inclusions, see Fig. 1.1. This composite inclusion model, which is discussed in detail in [10], is concisely summarized in this section. Each inclusion consists of a crystalline and an amorphous phase. A microstructural elasto-viscoplastic constitutive model is defined for both the crystalline and the amorphous phase.

The crystalline domain consists of regularly ordered molecular chains. The response of these domains is modelled as anisotropic elastic in combination with plastic deformation governed by crystallographic slip on a limited number of slip planes [2–13], which are shown in Fig. 1.1 and for which a rate-dependent crystal plasticity model is used. In the model, the plastic deformation rate is given by the summed contribution of all physically distinct slip systems:

$$\mathbf{L}_\mathrm{p} = \sum_{\alpha=1}^{N} \dot{\gamma}^\alpha(\tau^\alpha)\,\mathbf{P}^\alpha \tag{1.1}$$

where $\mathbf{P}^\alpha = \vec{s}^\alpha \vec{n}^\alpha$ is the Schmid tensor of the αth slip system, $\mathbf{L}_\mathrm{p}$ is the plastic velocity gradient tensor, and where the constitutive behaviour of the slip systems is defined by the relation between the resolved shear stress τ^α and the resolved shear rate $\dot{\gamma}^\alpha$, which is referred to as the slip kinetics.

The amorphous phase of semicrystalline polymeric material consists of an assembly of disordered macromolecules, which are morphologically constrained by the neighbouring crystalline lamellae. The elastic deformation of the amorphous domains is modelled by a generalized neo-Hookean relationship. Furthermore, a viscoplastic relation based on an associated flow rule is used, in combination with an eight-chain network model to account for orientation-induced strain hardening [14–16]. In particular, the viscoplastic behaviour of the amorphous phase is characterized by a relation between the effective shear rate and the effective shear stress $\dot{\gamma}^a(\tau^a)$, referred to as the yield kinetics of the amorphous phase.

The mechanical behaviour at the mesoscopic level is modelled by an aggregate of layered two-phase composite inclusions as was proposed by Lee et al. [6, 7] for rigid/viscoplastic material behaviour. Each separate composite inclusion consists of a crystalline lamella which is mechanically coupled to its corresponding amorphous layer. The stress and deformation fields

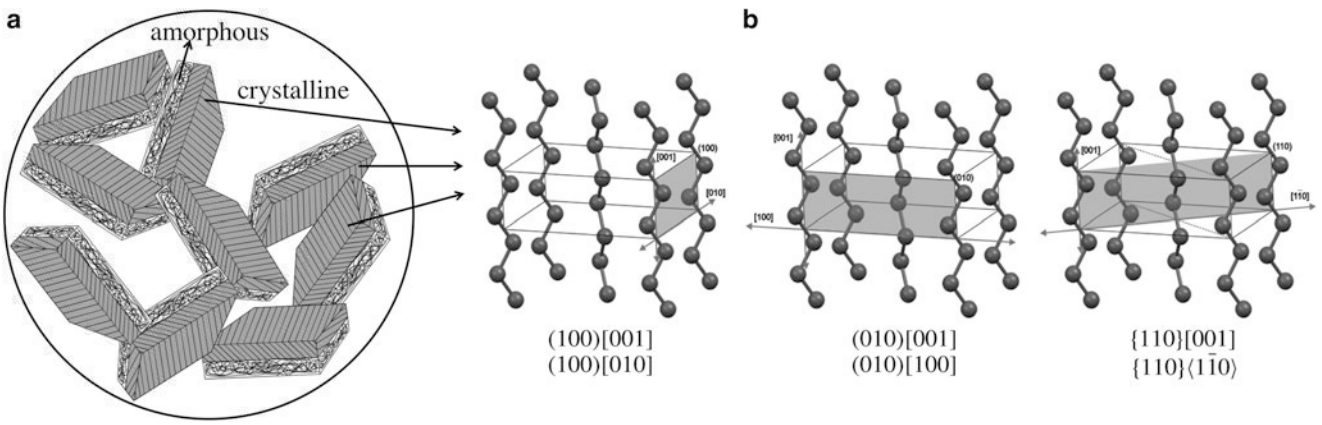

Fig. 1.1 (**a**) Aggregate of two-phase composite inclusions and (**b**) slip systems of the crystalline phase of polyethylene

within each phase are assumed to be piecewise homogeneous, however, they differ between the two coupled phases. The inclusion-averaged deformation gradient and the inclusion-averaged Cauchy stress are defined as the volume-weighted average of the respective phases. To relate the volume-averaged mechanical behaviour of each composite inclusion to the imposed boundary conditions for an aggregate of inclusions, a hybrid local–global interaction law is used [10].

1.3 Yield Stress and Time-to-Failure for Isotropic Material

In order to predict both the short- and long-term failure of polymers, quantitative predictions of the yield kinetics of these materials are required. The present work is directed towards the prediction of the yield and post-yield behaviour in semicrystalline polymers at different strain rates. A critical factor is the stress-dependence of the rate of plastic deformation, the slip kinetics, which is the mechanism underlying time-dependent, macroscopic failure. The kinetics of macroscopic plastic flow strongly depend on the slip kinetics of the individual crystallographic slip systems. Therefore, an accurate quantitative prediction requires a proper description of the rate-dependence of slip along crystallographic planes. As a first step in achieving this goal, an Eyring flow rule is used for each slip system [17, 18], see Fig. 1.2.

An activation energy is included in the slip kinetics in order to predict the temperature dependence of the kinetics of yield. In order to predict the response in both tension and compression, a non-Schmid effect (i.e. a dependence on the normal stress $\sigma_{\mathrm{n}}^{\alpha}$ acting on the slip system) is included in the slip kinetics [18], which for a single process is given by:

$$\dot{\gamma}^{\alpha} = \dot{\gamma}_0^{\alpha} \exp\left(-\frac{\Delta U^{\alpha}}{RT}\right) \sinh\left(\frac{\tau^{\alpha}}{\tau_0^{\mathrm{c}}}\right) \exp\left(\frac{\mu^{\alpha}\sigma_{\mathrm{n}}^{\alpha}}{\tau_0^{\mathrm{c}}}\right). \tag{1.2}$$

The yield kinetics of the amorphous phase is described with a similar relation, where instead of the non-Schmid effect, a pressure dependence is introduced.

The re-evaluation of the slip kinetics is performed using a combined numerical/experimental approach taking into account uniaxial compression and tension data of isotropic HDPE, for different strain rates and temperatures, see Fig. 1.3. The slip kinetics used to obtain these predictions were given in Fig. 1.2 (in absence of a normal stress on each slip system).

In Fig. 1.4, experimentally obtained data for the tensile yield kinetics and time-to-failure under creep conditions are shown for polyethylene, indicating the presence of a second processes, in addition to the α-relaxation mechanism, at higher temperatures. The kinetics of each slip system and the kinetics of the amorphous phase used in the model (as given in Fig. 1.2) account for both processes.

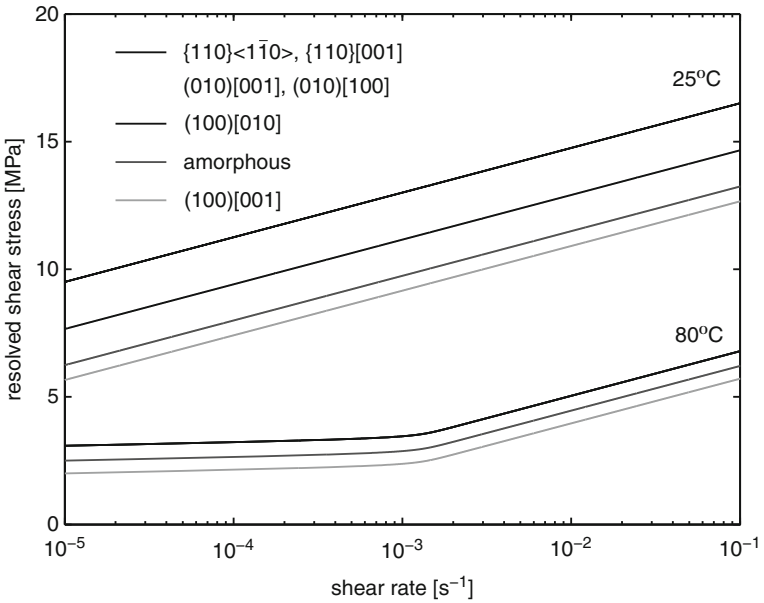

Fig. 1.2 Slip kinetics at different temperatures

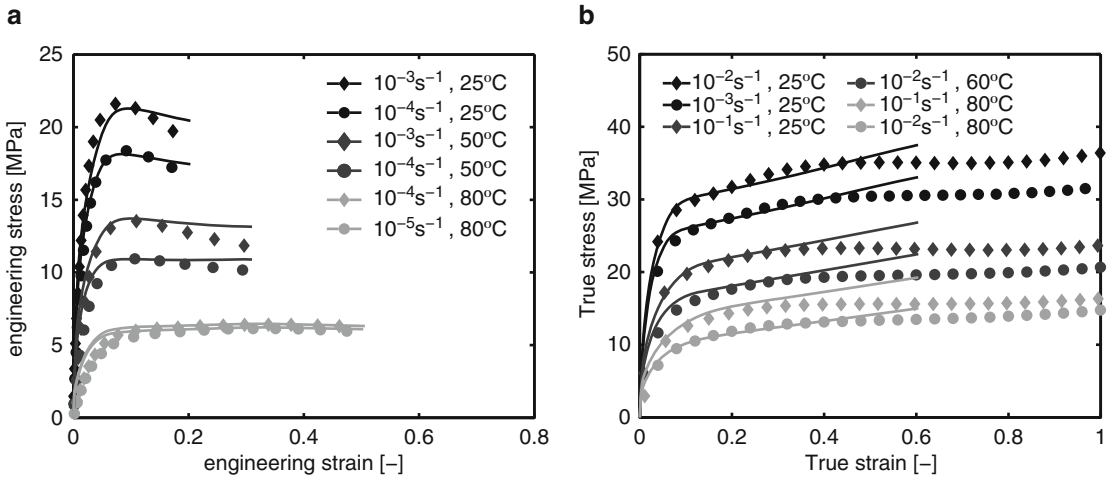

Fig. 1.3 (**a**) Tensile and (**b**) compressive response of isotropic HDPE. Markers indicate experimental results and lines are predicted by the micromechanical model [18]

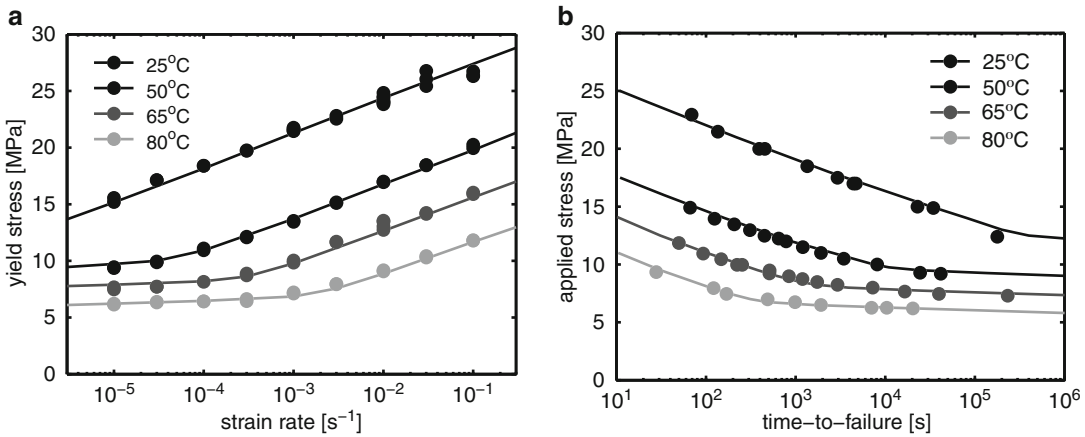

Fig. 1.4 Temperature dependence of (**a**) yield kinetics and (**b**) time-to-failure of HDPE in tension. Markers indicate experimental results and lines are predicted by the micromechanical model [18]

Also shown in Fig. 1.4 is a prediction of the temperature dependence of the macroscopic yield kinetics and time-to-failure with the micromechanical model with refined kinetics of crystallographic slip and deformation of the amorphous phase. Both the yield kinetics and time-to-failure of isotropically oriented material are described well by the micromechanical model for the range of temperatures and strain rates or applied loads, respectively.

1.4 Oriented Material

The mechanical response of extruded and drawn semicrystalline materials, in which a stacked lamellar morphology is commonly observed, depends on the direction of loading with respect to the direction of flow. Plastic deformation and failure are, therefore, both anisotropic. The predictive ability of the micromechanical model, including the characterization of the kinetics of crystallographic slip and amorphous yield based on isotropic material, is next evaluated for oriented high-density polyethylene. The initial morphology of the material is generated based on pole figures from wide-angle X-ray diffraction experiments, which show a strong alignment of molecular chains with the drawing direction for specimens produced with a large draw ratio ($\lambda = 6$), see Fig. 1.5.

Uniaxial loading of an aggregate of 500 composite inclusions with the orientation distribution shown in Fig. 1.5 and with slip kinetics as characterized for oriented material reveals slip activity on particularly the chain slip systems when the loading direction is aligned with the original drawing direction of the material [19]. In contrast, loading perpendicular to the

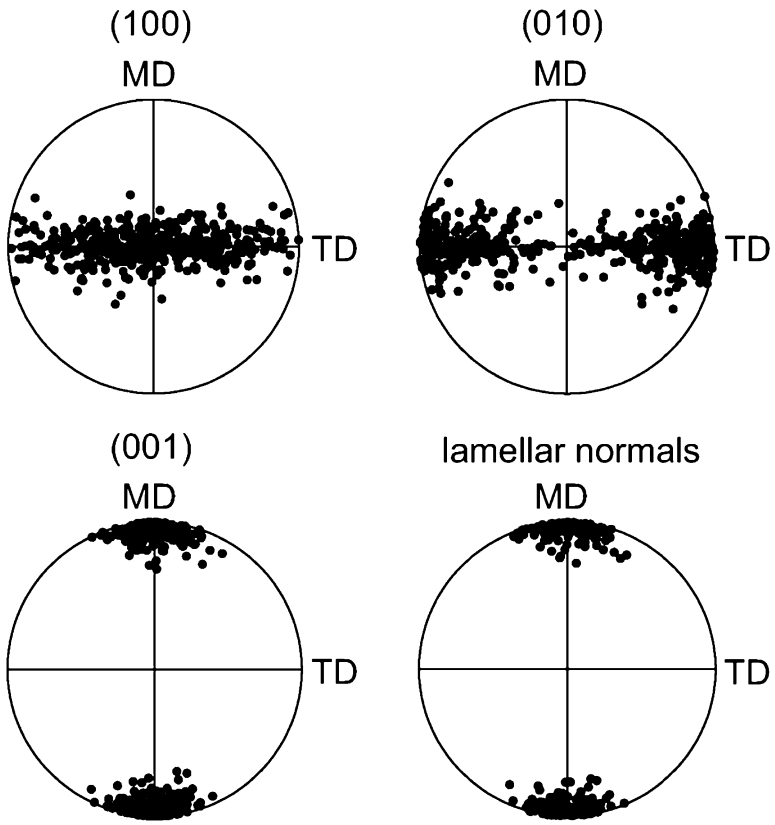

Fig. 1.5 Equal area projection pole figures of the principal crystallographic and lamellar orientation distributions for HDPE with a draw ratio of 6. The draw direction is vertical (MD)

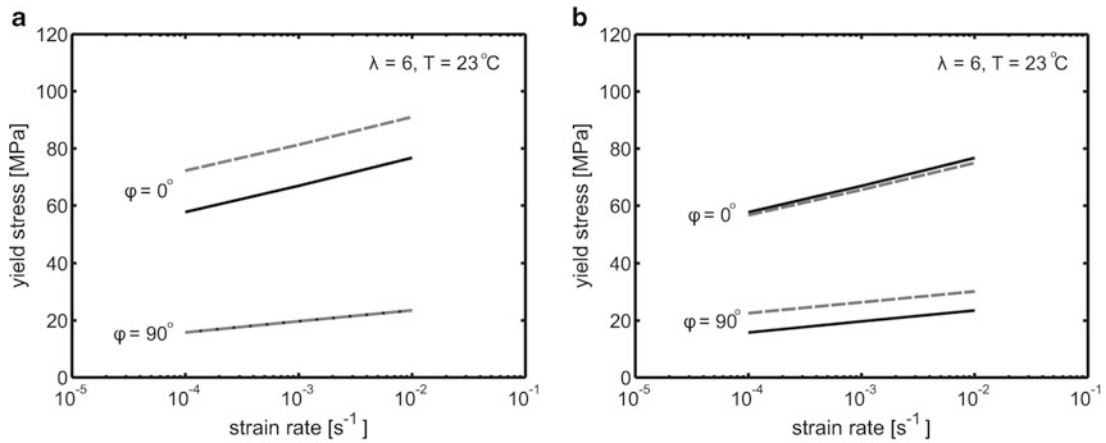

Fig. 1.6 The effect of modified slip kinetics on the yield stress for different loading angles [19]. Dashed grey lines show the model prediction corresponding to the modified kinetics and solid black lines give the prediction corresponding to the original kinetics (**a**) Modified chain slip kinetics, (**b**) modified transverse slip kinetics

original drawing direction leads to slip activity at macroscopic yield on transverse slip systems. Consequently, modifying the slip kinetics such that the chain slip systems have a larger shear yield stress for a given shear rate, affects the macroscopic response of the material when loaded in the original drawing direction, see Fig. 1.6a, which effectively leads to an enlarged macroscopic anisotropy. Analogously, increasing the transverse slip kinetic while keeping the chain slip systems unchanged

leads to an increased macroscopic yield stress when loaded in the transverse direction relative to the original loading direction, effectively decreasing the anisotropy of the material. This shows the potential of oriented systems for unambiguously determining the yield kinetics of individual slip systems. In doing so, however, also the presence of a potentially oriented amorphous phase should be dealt with. For more information, see [19].

1.5 Conclusions

The current research focuses on adding quantitative abilities to a micromechanical constitutive model for semicrystalline polymers, in particular for the stress-dependence of the rate of plastic deformation, referred to as the yield kinetics. A key issue in achieving that goal is the description of the rate-dependence of slip along crystallographic planes. The slip kinetics have been re-evaluated and characterized using a hybrid numerical/experimental procedure, based on the results of uniaxial compression and tension of isotropic HDPE, at various strain rates. The temperature dependence of the kinetics of yielding and time-to-failure are described well by the model.

The next step in this research on micromechanics of semicrystalline polymers is to validate the qualitative predictive capabilities for materials with oriented microstructures, which will behave anisotropically. This step might require a re-evaluation of the difference in kinetics between different slip systems, which cannot be distinguished based on isotropic microstructures. The potential of anisotropic systems for characterization of individual slip systems has been demonstrated. This step will be crucial for the use of such structure–property relationships for predicting performance and failure of polymer products. Furthermore, the model currently does not yet include the pronounced dependence on lamellar thickness that is experimentally observed and that may be included through the kinetics of crystallographic slip [20].

References

1. Lin L, Argon AS (1994) Structure and plastic deformation of polyethylene. J Mater Sci 29:294–323
2. G'Sell C, Dahoun A (1994) Evolution of microstructure in semi-crystalline polymers under large plastic deformation. Mater Sci Eng A 175:183–199
3. Parks DM, Ahzi S (1990) Polycrystalline plastic deformation and texture evolution for crystals lacking five independent slip systems. J Mech Phys Solids 38:701–724
4. Dahoun A, Canova R, Molinari A, Philippe MJ, G'Sell C (1991) The modelling of large strain textures and stress–strain relations of polyethylene. Textures Microstruct 14–18:347–354
5. Bartczak Z, Cohen RE, Argon AS (1992) Evolution of the crystalline texture of high density polyethylene during uniaxial compression. Macromolecules 25:4692–4704
6. Lee BJ, Parks DM, Ahzi S (1993) Micromechanical modeling of large plastic deformation and texture evolution in semicrystalline polymers. J Mech Phys Solids 41:1651–1687
7. Lee BJ, Argon AS, Parks DM, Ahzi S, Bartczak Z (1993) Simulation of large strain plastic deformation and texture evolution in high density polyethylene. Polymer 34:3555–3575
8. Nikolov S, Raabe D (2006) Yielding of polyethylene through propagation of chain twist defects: temperature, stem length and strain-rate dependence. Polymer 47:1696–1703
9. Gueguen O, Ahzi S, Makradi A, Belouettar S (2010) A new three-phase model to estimate the effective elastic properties of semi-crystalline polymers: application to PET. Mech Mater 42:1–10
10. Van Dommelen JAW, Parks DM, Boyce MC, Brekelmans WAM, Baaijens FPT (2003) Micromechanical modeling of the elasto-viscoplastic behavior of semi-crystalline polymers. J Mech Phys Solids 51:519–541
11. Van Dommelen JAW, Parks DM, Boyce MC, Brekelmans WAM, Baaijens FPT (2003) Micromechanical modeling of intraspherulitic deformation of semicrystalline polymers. Polymer 44:6089–6101
12. Van Dommelen JAW, Schrauwen BAG, Van Breemen LCA, Govaert LE (2004) Micromechanical modeling of the tensile behavior of oriented polyethylene. J Polym Sci, Part B: Polym Phys 42:2983–2994
13. Argon AS (1997) Morphological mechanisms and kinetics of large-strain plastic deformation and evolution of texture in semi-crystalline polymers. J Comput-Aided Mater Des 4:75–98
14. Arruda EM, Boyce MC (1993) A three-dimensional constitutive model for the large stretch behavior of rubber elastic materials. J Mech Phys Solids 41:389–412
15. Boyce MC, Montagut EL, Argon AS (1992) The effects of thermomechanical coupling on the cold drawing process of glassy polymers. Polym Eng Sci 32:1073–1085
16. Boyce MC, Parks DM, Argon AS (1988) Large inelastic deformation of glassy polymers. part I: rate dependent constitutive model. Mech Mater 7:15–33
17. Sedighiamiri A, Govaert LE, Van Dommelen JAW (2011) Micromechanical modeling of the deformation kinetics of semicrystalline polymers. J Polym Sci, Part B: Polym Phys 49:1297–1310

18. Sedighiamiri A, Govaert LE, Kanters MJW, Van Dommelen JAW (2012) Micromechanics of semicrystalline polymers: yield kinetics and long-term failure. J Polym Sci, Part B: Polym Phys 50:1664–1679
19. Sedighiamiri A, Govaert LE, Senden DJA, Van Dommelen JAW A micromechanical study on the deformation kinetics of oriented semicrystalline polymers, in preparation
20. Argon AS, Galeski A, Kazmierczak T (2005) Rate mechanisms of plasticity in semicrystalline polyethylene. Polymer 46:11798–11805

Chapter 2
Stress-Relaxation Behavior of Poly(Methyl Methacrylate) (PMMA) Across the Glass Transition Temperature

Danielle Mathiesen, Dana Vogtmann, and Rebecca Dupaix

Abstract Characterizing Poly(methyl methacrylate) (PMMA) across its glass transition temperature is essential for modeling warm deformation processes such as hot embossing. Its mechanical properties vary significantly across the glass transition as well as with strain rate. Several previous models have attempted to capture this behavior utilizing uniaxial compression experimental data with limited success. In this work, compression experiments including stress relaxation at large strains are conducted to aid researchers in developing better models. Multiple temperatures, final strains, and strain rates are examined to characterize the material across values found in typical hot-embossing processes. It was found that the amount of stress relaxed is highly dependent on the temperature and strain at which it is held. With this data, a model can be developed that will accurately capture stress relaxation with the final goal of being able to simulate hot embossing processes.

Keywords PMMA • Glass transition • Stress relaxation

2.1 Introduction

Hot embossing or nanoimprint lithography is a process that is used to impose micro- and nano- scale surface features on a polymer. Applications of hot embossing include the molding of microchannels or optical arrays [1]. The polymer is heated past its glass transition temperature, T_g, and a finite deformation is applied to the stamp. For a period of time, this position is held at the original elevated temperature, allowing the polymer to flow and fill in the stamp. Next, it is cooled and unmolded simultaneously as shown in Fig. 2.1. The inherent sensitivity of the polymer's mechanical behavior near the glass transition combined with the many process variables involved make predicting the process outcome challenging. Polymers are known to be highly sensitive to both temperature change and strain rate near the glass transition. In addition, the final strain and hold time during the process significantly affect the outcome [2]. As a result, it is difficult and expensive to develop an optimized process through experiments alone and a predictive material model has the potential to greatly improve the process. Hot embossing is already embraced as a low-cost environmentally friendly fabrication technique and the ability to optimize the process will only increase its attractiveness.

At the conditions at which hot embossing is performed, polymers are highly sensitive to strain rate and variation of temperature [2]. One polymer commonly used in hot embossing is Poly(methyl methacrylate) (PMMA). PMMA is an amorphous thermoplastic with a glass transition temperature of approximately 105–110 °C that makes it ideal for the process of hot embossing [3]. While previous experiments have shown that its capability in hot embossing [1, 3], optimization of the fabrication technique is challenging to develop a large-scale production of these devices. Several models have been developed to try and capture the behavior of PMMA around glass transition temperature [4–8]. The majority of the models developed have been based on uniaxial compression experiments [4–7]. While the models are largely able to capture the behavior in uniaxial compression, they are still unable to predict the correct amount of spring-back present in hot embossing. It is believed that they fail to capture the behavior because none adequately capture stress relaxation of the polymer.

Stress relaxation is present in the process of hot embossing during the hold period after the deformation is applied. To accurately design a model, experimental stress relaxation data of PMMA in compression at small and large strains is needed.

D. Mathiesen • D. Vogtmann • R. Dupaix (✉)
Scott Laboratory, The Ohio State University, 201 West 19th Ave, 43210 Columbus, OH, USA
e-mail: dupaix.1@osu.edu

B. Antoun et al. (eds.), *Challenges In Mechanics of Time-Dependent Materials and Processes in Conventional and Multifunctional Materials, Volume 2*, Conference Proceedings of the Society for Experimental Mechanics Series,
DOI 10.1007/978-3-319-00852-3_2,

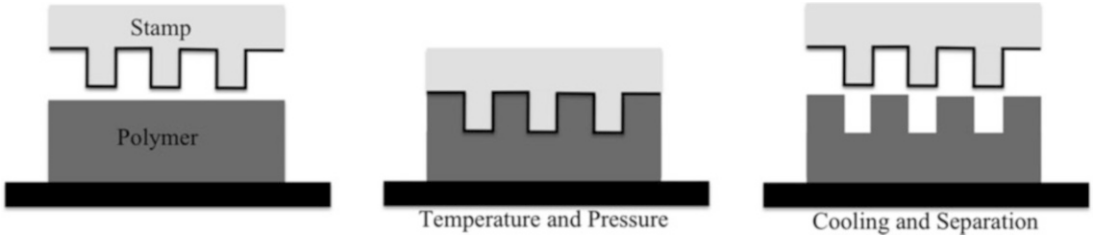

Fig. 2.1 (**a**) The polymer and stamp are heated to a temperature above glass transition (**b**) The stamp is lowered and pressure is applied to the polymer forcing the polymer to flow and fill in the voids (**c**) The polymer and stamp are cooled briefly while still in contact then separated with cooling continuing

The majority of stress relaxation data available on PMMA is based on the works of McLoughlin and Tobolsky that found a master relaxation curve for PMMA at small tensile strains [9]. Others have also performed stress relaxation experiments on PMMA at small tensile strains [8], multiaxial compression [10], and torsion [11] but little to no data is found at large compressive strains during relaxation. It is important to study the relaxation behavior of PMMA at large compressive strains because in hot embossing, large local compressive strains will occur that need to be accurately captured during a finite element simulation. The purpose of these experiments is to provide necessary data to quantify the amount of stress relaxation present in PMMA at temperatures, strain rates, and final strains found in hot embossing to better predict the spring-back.

2.2 Experimental

PMMA cylinders were cut from commercial sheet stock supplied by Plaskolite, Inc. to an initial height and diameter of 8.8 and 10 mm respectively. An Instron 5869 screw driven materials testing system was used in conjunction with an Instron 3119–409 environmental chamber to heat the samples to the specified temperature. An Instron 5800 controller running Instron Bluehill software controlled the load frame. Displacement of the upper compression plate was controlled and the force recorded with a 50 kN load cell. Using the displacement and force data, true stress and true strain were calculated, using the initial dimensions of the sample and the assumption that volume remained constant. Samples were tested using a ramp-hold loading history, where the ramp was a constant true strain rate followed by a hold at a specific final strain. Two loading strain rates (−1.0/min and −3.0/min), three final true strains (−0.5, −1.0, −1.5) and five temperatures (95–135 °C) composed the testing matrix. All samples were placed in a dessicant chamber at least 24 h prior to the test to control the amount of moisture present. Teflon sheets were placed between the compression plates and sample to reduce friction. WD-40 was applied between the compression plates and Teflon film to provide additional lubrication. Each sample was placed in the pre-heated environmental chamber for 30 min prior to testing to ensure the entire sample was at the testing temperature. To ensure repeatability, each test was run twice.

2.3 Results

At temperatures less than T_g PMMA behaves as a viscoelastic solid. There is an initial region of elastic behavior followed by a small period of strain softening as evident in Fig. 2.2. The strain softening is attributed to aging of the polymer, which decreases the free volume of the polymer and thereby causes an elevated yield stress at small strains. If the polymer were heated past T_g and quenched the free volume would increase and the strain softening would no longer be present [12]. As the temperature is increased the strain softening effects diminish and are no longer present at temperatures greater than T_g as shown in Fig. 2.3. Another temperature dependent region is the elastic portion at small strains. When the temperature is greater than transition, the elastic region essentially disappears and the polymer behaves more fluid-like. After the initial yield, the material begins to exhibit strain hardening attributed primarily to molecular orientation. At higher temperatures, the amount of strain hardening decreases as shown in Fig. 2.4.

During the hold period, stress relaxation occurs and is highly dependent on temperature and the strain at which it is held. At temperatures less than T_g there is a large initial drop in the stress. After this initial drop, the polymer continues to relax, although the rate of relaxation remains at a lower, more constant rate. At temperatures near the glass transition, there is still a small region of an initial drop once the hold period begins, however it is less severe than at lower temperatures. Similar to the

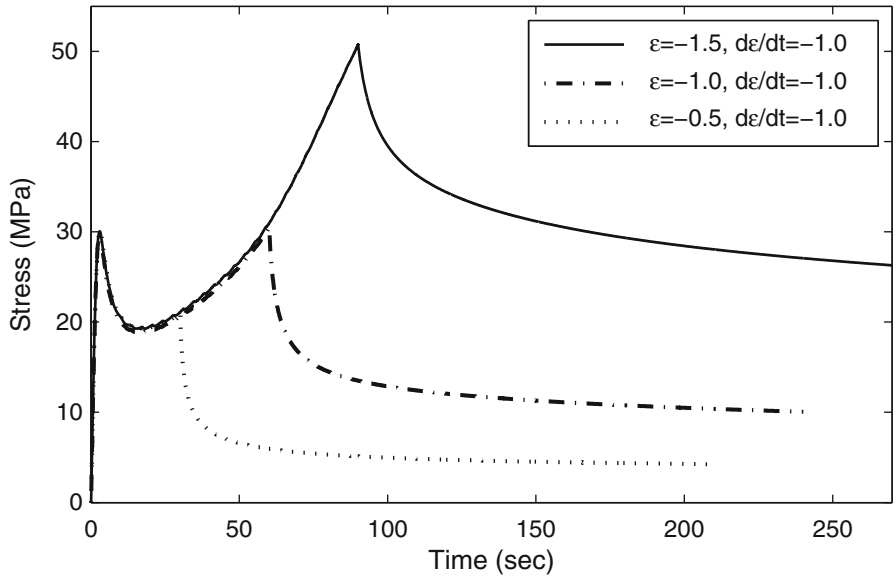

Fig. 2.2 Stress versus time at 95 °C for samples loaded at a rate of −1.0/min and held for 180 s. Each sample was held at a different final strain: −0.5, −1.0, and −1.5

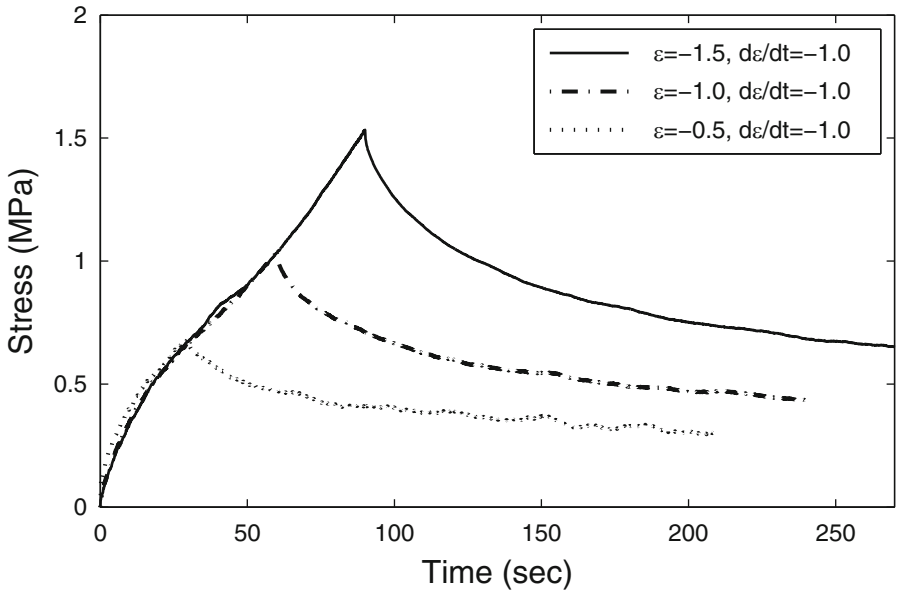

Fig. 2.3 Stress versus time at 135 °C for samples loaded at a rate of −1.0/min and held for 180 s. Each sample was held at a different final strain: −0.5, −1.0, and −1.5

low temperatures, it reaches a smaller, more constant relaxation rate after this initial drop. Much less of an initial drop is present in the stress at the beginning of the hold period at temperatures greater than transition. For a given held strain and temperature, strain rate does not affect the final relaxation value. As shown in Figs. 2.5, 2.6 and 2.7 the higher strain rate values cause a larger initial drop in the stress than a lower strain rate at the same held strain. However, the steady stress it relaxes to is approximately the same as its lower strain rate counterpart.

To quantify the amount of stress-relaxation, the percent relaxed is calculated to give an idea of relative relaxation amounts. The percent relaxed is calculated for each temperature and held strain by subtracting the steady relaxation stress from the maximum stress achieved before the hold period and dividing by the maximum stress. At temperatures less than